Effect of Carburization on the Residual Stress and Fatigue Life of a Transmission Shaft

Shun Zhang
Central Manufacturing Engineering, GM Powertrain, Ypsilanti, MI, USA

Zhichao Li, B. Lynn Ferguson
Deformation Control Technology, Inc. Cleveland, OH, USA

Abstract

The application life of many key automotive powertrain components, such as shafts, is closely related to their heat treatment properties, most importantly the residual stress profile. Heat treatment parameters, such as carburization time and temperature, as well as quenching conditions affect the residual stress distribution along the shaft. One method of optimizing the heat treatment parameters to achieve the best residual stress profile is conducting repeated heat treatment trials and residual stress measurements. An alternative, less costly method of improving the heat treatment process to obtain improved part performance is using computer simulation. In this study, the residual stress state due to carburization and quench hardening of a transmission output shaft was simulated using a commercially available heat treatment simulation software package, DANTE.

In addition to the residual stress prediction, hardness, volume fraction of metallurgical phases, and shaft distortion are predicted. Efforts were initiated to validate the modeling work, which includes the measurement of the carbon profiles and the residual stress distributions. Eventually, the modeling capability will be used to optimize the residual stress profile and the corresponding fatigue life by controlling the carburization schedule. As the first part of this study, the carbon distributions and residual stress profile simulated with different carburization schedules are presented in this paper.

Introduction

Distortion of components due to heat teatment and other process steps is important to the automotive powertrain manufacturer because of the added cost of correcting distortion problems. Distortion due to heat treatment can be minimized by tuning the heat treatment process parameters, such as the heating and cooling rates, the carburization schedule, etc. The durability of some critical transmission components, such as shafts, depends largely on their heat treated properties, with surface residual stress being especially important to fatigue life. The optimization of heat treatment parameters to achieve shaft durability is greatly helped by using sn accurate computer simulation tool, DANTE®.[1-3]

Heat treatment results that are of common interest include the volume fractions of phases, hardness, residual stress profile, and part distortion. Heat treatment is a transient thermal process, and most of these results can only be measured after heat treatment has been completed. The thermal gradient during both heating and cooling works together with the phase transformations to continually change the internal stress and deformation of the part being heat trteated. The material response of a specific part during the heat treatment process is difficult to document just using these final measurements. The development of heat treatment simulation software makes it possible to understand the material response during the heat treatment process, including the evolution of internal stresses and deformation, the phase transformation sequences, and the probability of cracking.[1-7] DANTE is a commercial heat treatment software tool based on the finite element method that has been used to predict steel phase transformations, dimensional change, residual stress, and hardness for heating, carburization, cooling, and tempering processes.[6] Computer simulation has increased the level of understanding of heat treatment processes because the events that occur during heating and cooling can be accurately modeled. In turn, advances in computer hardware, in combination with accurate simulation, has made the design and optimization of the heat treatment processes more cost effective than traditional experimental trial-and-error methods.

By increasing the carbon content of an alloy steel, the diffusive transformations will be retarded, and the martensitic phase transformation starting temperature will be depressed. As a combined effect of the thermal gradients and phase transformation sequences, quenching a carburized steel part normally will generate compressive residual stresses in the carburized case. However, the relations among the the carburization schedule, residual stress state, and fatigue life are not well understood quantitatively. This paper applies heat treat simulation to investiagte the effect of different carburization schedules on the residual stress, distortion, and fatigue life of a shaft component. The validation of these simulation results will be completed in the second part of this project.

Shaft Modeling and Material Characterization

Finite Element Modeling

The geometry of the half-section of the transmission output shaft modeled in this study is shown in Figure 1(a). The shaft is approximately 350 *mm* in length, and it has a centrally located blind bore that runs about half the shaft length. It has six oil holes that intersect the blind bore, four on one side of the shaft barrel and two on the opposite side. The output shaft has a longitudinal symmetry plane, and the center lines of the six oil holes are located in this plane. In this study, the half symmetry of the shaft was used for the finite element simulations. The finite element mesh is shown in Figure 1(b). Fine surface elements were defined adjacent to all the outer and inner surfaces to accurately capture the surface thermal and carbon gradients. The finite element mesh includes 61,915 hexahedral elements and 68,582 nodes. Point A and point B in Figure 1(a) and the location inside the circle in Figure 1(b) are referred to later in this paper.

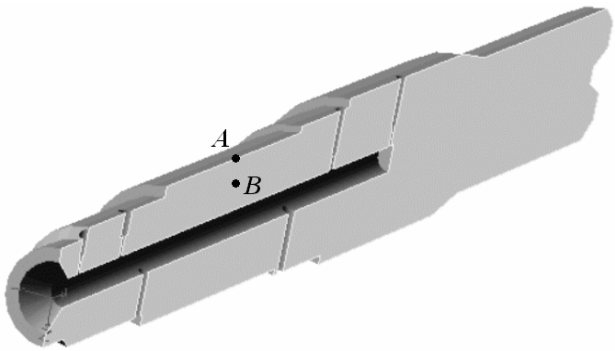

(a)

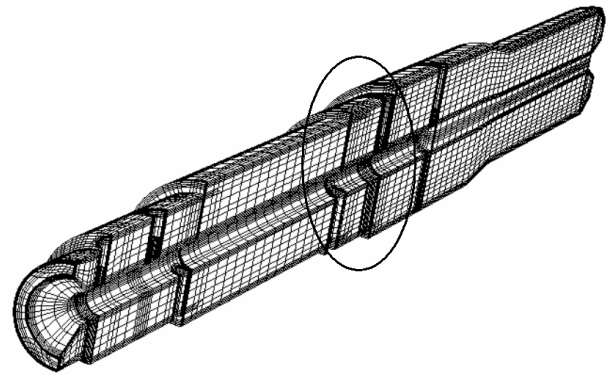

(b)

Figure1: (a) Half Geometry of the Transmission Output Shaft, (b) Finite Element Meshing Used for Simulations.

Material Characterization

This transmission output shaft is made of SAE 8620 steel. The heat treatment process includes furnace heating, carburization, transfer from the furnace to a quench tank containing molten salt at 212º C, and air cooling to room temperature. Four different carburization schedules were studied, and they were 3 hours, 8 hours, 12 hours, and 18 hours carburization time at 927º C, with an atmosphere carbon content of 0.9%. In this study, all the other heat treatment process steps were held constant to fully study the effect of the carburization process and the resultant carbon profile on the phase transformation and internal stress histories.

The phase transformations play a key role during the steel heat treatment process. To model the heat treatment of the transmission output shaft, the phase transformation kinetics parameters, thermal properties and mechanical properties of SAE 8620 steel during both heating and cooling processes for different carbon levels are required. The DANTE database includes the phase transformation kinetics for heating, cooling and tempering of this carburized steel. The individual phases for SAE 8620 include austenite, ferrite, bainite, martensite, and tempered martensite. The accuracy of the heating and cooling kinetics directly affects the accuracy of the predicted distortion and residual stress distribution. The yield stress of austenite is low at high temperature. Therefore, the shaft is under low stress, but more typically is stress free, at the austenitization temperature. As a result, the quenching step contributes more to the final residual stress distribution than the heating step. However, the effect of heating on part distortion may be significant, and it depends on the temperature and phase transformation uniformity. [2]

DANTE provides a utility to check the accuracy of the diffusive transformation kinetics during cooling by generating the time-temperature-transformation (TTT) diagram from the model kinetics parameters. Figure 2(a) and Figure 2(b) show the TTT diagrams for austenite decomposing to bainite for 0.2% carbon and 0.8% carbon levels, respectively. These curves were generated by the DANTE utility solely for the purpose of checking the kinetics parameters, and these curves are not used directly during the heat treatment simulations. By increasing the carbon content, the bainite transformation is retarded. As shown in Figure 2(a), the bainite transformation for 0.2% carbon begins after a 2 second hold at just above 500º C, and the transformation is completed in 20 seconds. For 0.8% carbon, the transformation begins after about 30 seconds at 500º C, and it is completed after about 300 seconds. The martensite transformation starting temperature decreases with the increase of carbon content. During DANTE simulations, the bainite transformation is still active when the temperatures are below the martensitic transformation starting temperature. The salt bath temperature is below the *Ms* of the base 8620 steel. However, the salt bath temperature is higher than the *Ms* of 8680, which is the high carbon case metal. The 8620 carburized shaft will go through a competition between bainite and martensitic transformations during the salt bath quench period.

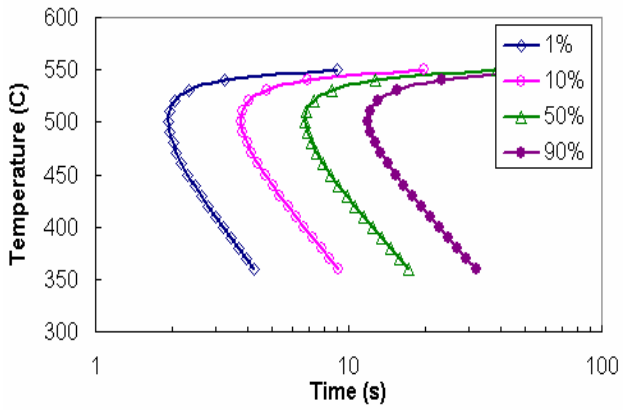

(a)

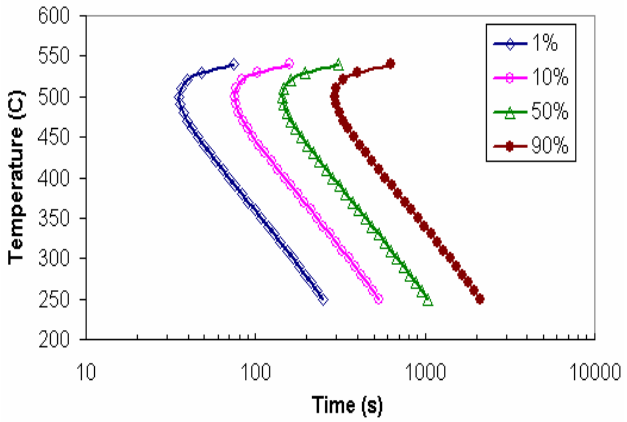

(b)

Figure2: TTT Diagrams of SAE 86XX Generated from DANTE Utility: (a) 0.2% Carbon, (b) 0.8% Carbon.

The thermal and mechanical properties are also required to simulate the heat treatment process beyond the phase transformation kinetics. All the thermal and mechanical properties are based on individual phases and carbon levels. These data are available in DANTE database for 86xx steel.

Results and Discussions

Modeling of Carburization Process

The carburization process is used to improve the surface hardness and strength of steel components, as well as to generate compressive residual stress in the carburized case during quenching. The values and profile of the residual stress in the surface are directly related to the transmission output shaft's fatigue life. In this study, three critical sections were selected to investigate the carbon distribution generated by different carburization schedules, as well as the effect of the carbon profile on the residual stress and phase distributions. All three sections are located in the symmetric plane as shown in Figure 1(a). The location inside the circle in Figure 1(b) is magnified and shown in Figure 3.

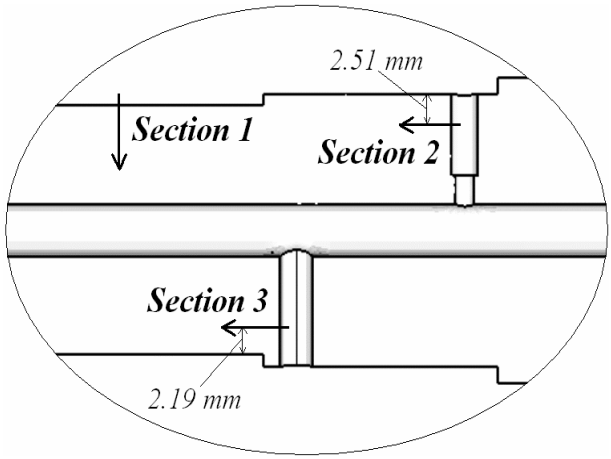

Figure 3: Three Critical Sections of the Transmission Output Shaft Used to Evaluate the Heat Treatment Results.

Section 1 is a straight line pointing vertically from OD surface of the shaft to the inside, as shown in Figure 3. Carbon profiles for this section represent the general shaft OD surface profile. Sections 2 and 3 are located at two oil holes. Sections 2 and 3 are parallel to the axis of the shaft, and they point from the oil hole surfaces into the interior. The sections 2 and 3 are *2.51 mm* and *2.19 mm* away from the shaft OD surface, respectively, as shown in Figure 3. The distances of these two sections from the OD surface of the shaft were simply determined from the finite element model, which are represented by two lines of nodes. Section 2 and section 3 have high cracking possibility during torsional loading.

The carburization times for the four schedules were 3, 8, 12, and 18 hours, respectively. The carburization temperature was 927º C and the atmosphere carbon potential was 0.9% in all cases. Figure 4(a) shows the predicted carbon profiles at the shaft OD, section 1, for the four carburization schedules. The X-axis in Figure 4(a) is the depth in *mm* from the OD surface of the shaft, and the Y-axis is the weight fraction of carbon. By increasing the carburization time, the surface carbon content increases and the case depth is deeper, as shown in the Figure 4(a). The depths for a 0.4% carbon level for the four carburization schedules are 0.8 *mm*, 1.1 *mm*, 1.4 *mm*, and 1.7 *mm*, respectively. From Figure 4(a), carburization times of 12 or more hours produce carbon profiles that extend at least 3 mm below the OD surface. Figure 4(a) also shows that the carbon gradient in the case decreases with the increase of the carburization time. The carbon gradient is the driver of the carbon diffusion process. The carbon diffusion rated will drop with the decrease of the carbon gradient (the increase of the carburization time). Therefore, the case depth does not increase linearly with the carburization time. Heat treaters normally try to minimize the time needed to meet the specified case depth.

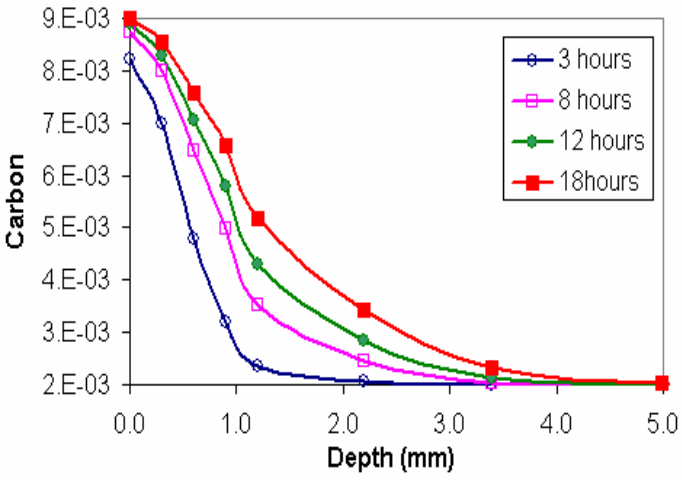

(a)

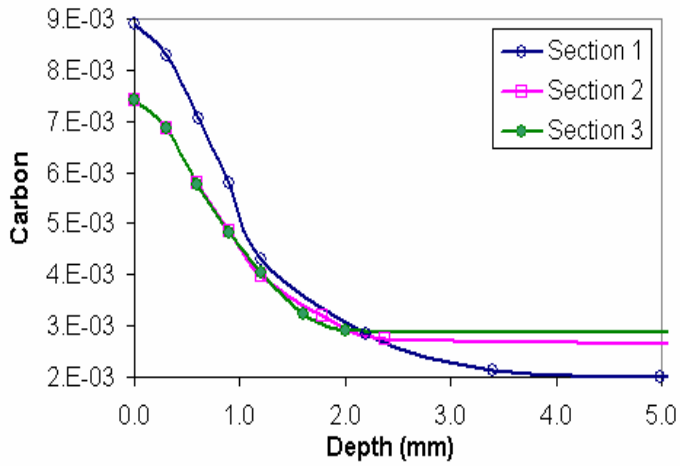

(b)

Figure 4: Weight Fraction of Carbon: (a) Various Carburization Times at Section 1, (b) at Three Critical Locations with 12 Hours Carburizing.

Figure 4(b) shows the carbon distributions at the three critical sections with 12 hours carburization time period. The X-axis in Figure 4(b) is the depth along the three sections from the respective surfaces. Sections 2 and 3 have lower surface carbon content than section 1. Sections 2 and 3 have similar carbon distribution profiles. The difference of the carbon distributions between section 1 and sections 2 and 3 comes from two reasons: the difference in local carbon potential of the gas atmosphere, and the geometrical effect. During the carburization process, the gas carbon content inside the oil holes was lower than the regular gas carbon content because of the gas flowing pattern. This statement is based on experience with similar parts. A convex geometry has a higher surface to mass ratio than a concave geometry. The carbon content in a convex surface is usually higher than the carbon content in a concave surface during the same carburization schedule. The carbon contents of sections 2 and 3 do not drop down to the base carbon level because these two sections are close enough to the shaft OD surface that carbon diffusion from the OD surface affects the values in sections 2 and 3.

Modeling of Phase Transformations and Stress Evolution

Heat treatment is a transient process. During heat treatment, the thermal gradient and phase transformations work together to alter the internal stress state and local dimensional changes. In this study, two critical points were selected to investigate the cooling history, phase transformation sequences, and the generation of internal stress during the salt quenching process. The two points are points A and B as shown in Figure 1(a). Point A is located on the shaft OD surface, and point B is located in the core of the shaft.

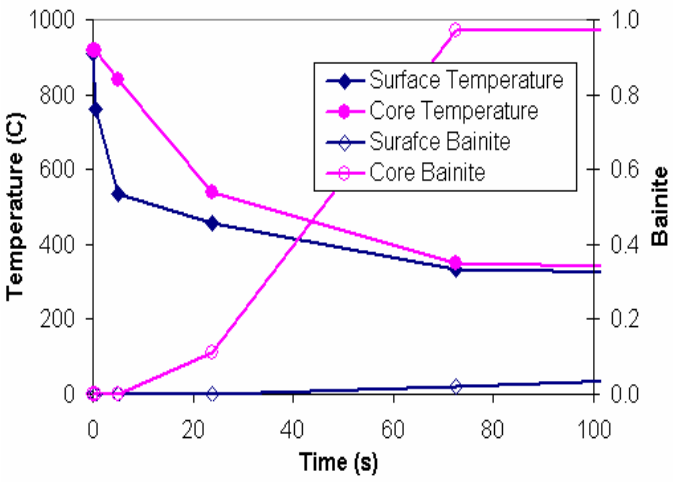

(a)

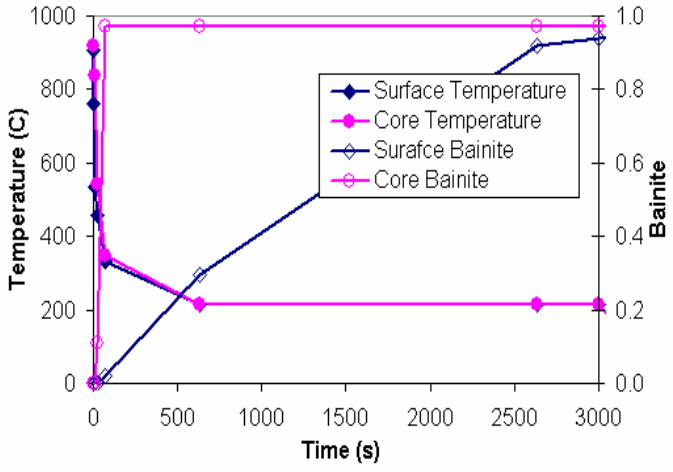

(b)

Figure 5: Comparison of Temperatures and Bainite Phase Transformation Histories between a Surface Point and a Core Point: (a) over the first 100 seconds of Salt Quench, (b) over a Period of 3000 Seconds.

Figure 5 shows the temperature difference and the bainite phase transformation histories at these two points during quenching. In Figure 5(a), the X-axis is the time started at the

beginning of quenching. The curve with solid diamond marks represents the temperature history of the surface point (point A in Figure 1(a)). The curve with solid circle marks represents the cooling of the core point (point B in Figure 1(a)). As expected, the surface point cools faster than the core point at the beginning of the salt quenching process. After 70 seconds in salt bath, the temperature difference between the surface point and the core point becomes negligible and the shaft cools uniformly until it reaches the salt bath temperature. The surface point has 0.85% carbon, and the core point has a base carbon level of 0.2%, as derived from Figure 4(a). The high carbon content at the OD surface delays the formation of bainite in comparison to the core, as shown by the bainite TTT diagrams in Figure 2. Because of the carbon content difference, the bainite formation rate at the surface point is slower than the core point even though the cooling rate at the surface point is faster. In Figure 5(a), the curve with hollow circle marks is the volume fraction of bainite in the core in terms of the quenching time. The bainite transformation was completed in about 70 seconds in the core, Point B. The curve with hollow diamond marks represents the volume fraction of bainite at the OD surface, Point A. At 70 seconds of salt quenching, less than 5% bainite was predicted to have formed at the surface, Point A. Figure 5(b) shows temperature and bainite volume fraction for quenching time up to 3000 seconds. After 3000 seconds, the bainite transformation at the surface point is still not completed. In practice, the goal is to complete the bainite transformation at the surface point, and a longer time in the salt bath is used.

During the salt quenching process for this transmission output shaft, the thermal gradient and phase transformations both contributed to the internal stress evolution. By comparing the same surface and core points, A and B, Figure 6 shows most of the hoop stress history during the quenching process; the quickly changing events in the first seconds of the quench are not evident in Figure 6. The early, rapid changes in stress are described in the following sentences. The surface temperature dropped faster than the core temperature over the first 15 to 20 seconds of the quenching process, and the thermal contraction of austenite at the surface generated surface tensile stress. To balance the surface stress, the core was under compression over this period. The surface tensile stress generated localized plastic deformation to relieve the tension because of the low yield stress of austenite. At about 12 seconds of quenching, the temperatures at the surface and core points reached the maximum difference, as shown in Figure 5(a). Between 12 seconds and 70 seconds, the cooling rate at the core point was faster than the cooling rate at the surface point, which generated tensile stress in the core. At the same time, the bainite formation in the core generated compressive stress in the surface because of the volume expansion caused by bainite formation. A small volume fraction of martensite, i.e. < 10%, was formed in the carburized case simultaneous to bainite forming in the core. Therefore, the changes in stress state in the early stages of quenching are complicated because the thermal gradient and phase transformation act in combination to affect the internal stress and accompanying dimensional changes.

After 70 seconds, the temperature of the shaft became more uniform, and Figure 5(a) shows that the bainite transformation in the core is nearly completed. The martensitic transformation in the carburized case stopped once the shaft temperature reached the salt bath temperature. Figure 5(b) shows that the bainite transformation in the carburized case became the dominant event over the remaining several thousand seconds. The material volume in the case expanded with the formation of bainite, and, as a result, the stress in the carburized case shifted from tensile stress to compressive stress, while the stress at the core shifted to tensile stress, as shown in Figure 6. The internal stress changes in Figure 6 show how the surface compressive residual stress was generated during the quenching process of carburized steel parts.

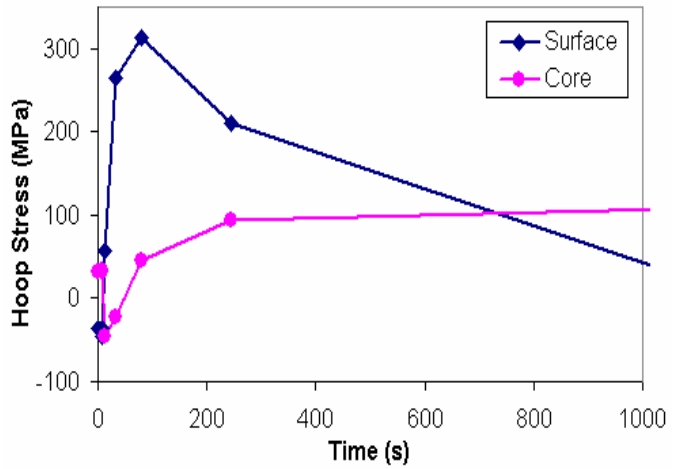

Figure 6: Comparison of Hoop Stress Updating between a Surface Point and a Core Point.

During the salt quench process of this transmission output shaft, the cooling rate is fast enough to miss the ferrite and pearlite transformation nose. Therefore, there is no ferrite and pearlite formation during the entire cooling process. Martensite and bainite are the only two phases formed from austenite during salt bath quenching. Figure 7 shows the predicted bainite distribution at the end of the heat treatment process for a shaft that was carburized for 12 hours. The core of the shaft, with the base carbon content of 0.2%, transformed to 100% bainite during quenching. As mentioned above, the increase in carbon content decreases the martensitic transformation starting temperature (*Ms)*, with the *Ms* of 8620 being about 415º C and the *Ms* of 8680 being about 205º C. The salt bath temperature is 212º C. The carbon content at the shaft OD surface is about 0.85%, which means that there is no martensite transformation during salt quenching and holding period in this highest carbon location. The high carbon austenite at the surface transforms to bainite during the isothermal holding period. Some retained austenite at the

surface after isothermal holding will transform to martensite during the air cool process. The carbon content at the core has a base carbon content of 0.2%, so any regions with carbon levels below about 0.7% have the possibility of forming martensite during cooling in the salt bath. Because the bainite formation rate is very fast for the base carbon level of 0.2%, 100% bainite will be formed before the temperature of the shaft reaches the salt temperature. In the carburized case, the martensitic and bainite phase transformations compete with each other. For a 12 hour carburization time, the volume fraction of bainite near the surface is above 90% during isothermal holding in the salt bath. At a depth of 1.0 *mm* from the OD surface of the shaft where the carbon level is approximately 0.55%, about 40% martensite was formed during salt cooling, as shown in Figure 7. The carburization schedules have a significant effect on phase transformations and final phase distributions.

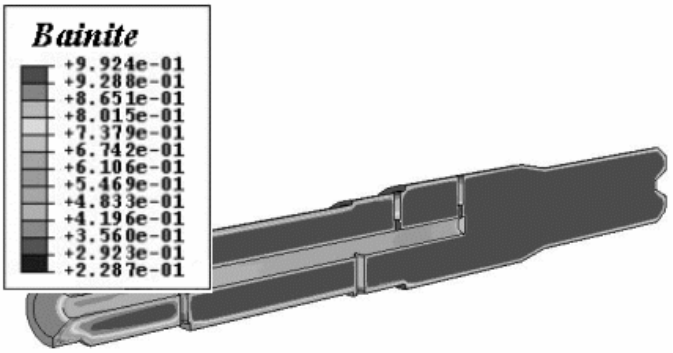

Figure 7: Contour of Bainite Distribution at the End of Heat Treatment with 12 Hours Carburization Time.

The effect of carbon content on the martensite and bainite phase distributions is also shown in Figure 8. At the OD surface of the shaft, there are about 7% martensite and 93% bainite predicted after the heat treatment. The bainite was formed during the isothermal holding process in the salt bath. The carbon content at the OD surface is about 0.85%, which is shown in Figure 4(a). After isothermal holding in the salt bath, about 7% retained austenite was left at the surface. The austenite remaining after the quench will transform to martensite during the following air cooling step. Figure 8(a) shows the martensite and bainite distributions along section 1 with different carburization schedules. The X-axis is the depth in *mm* from the OD surface of the shaft. The volume fraction of martensite increases with the depth first, and then decreases after a peak. With 3 hours carburization time, the martensite peak locates at a depth of 0.5 *mm*, and the volume fraction of the martensite peak is about 30%. The profile of the bainite distribution is opposite to that of the martensite distribution. By increasing the carburization time, the martensite peak shifted to a deeper location. The difference of the phase distributions between 12 and 18 hours carburization time is not significant. For both carburization cases, the volume fractions of the martensite peak are about 40%, and the depths of the peak are about 1.0 *mm*.

Figure 8(b) shows the martensite and bainite distributions along the three critical sections from the carburization schedule of 12 hours holding time period. Among the three critical sections, the section 1 has a martensite peak of about 0.9 *mm*. The sections 2 and 3 have the same martensite peak of about 0.6 *mm.* The martensite peak difference between the section 1 and sections 2 and 3 is caused by the deeper carburized case along the section 1.

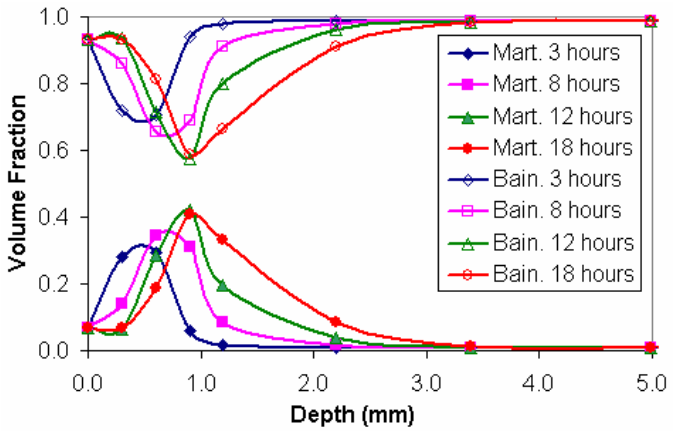

(a)

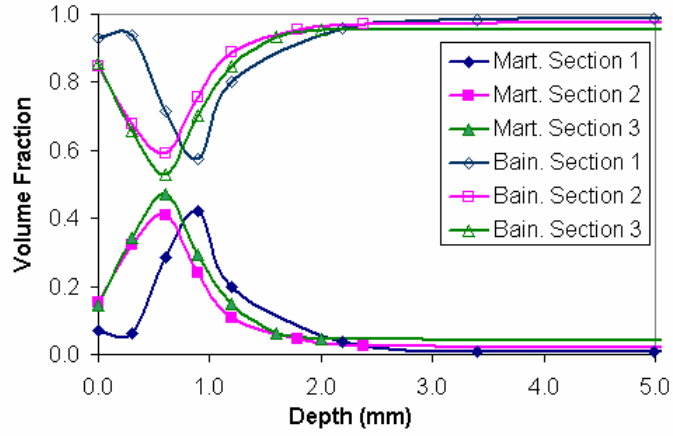

(b)

Figure 8: Volume Fractions of Bainite and Martensite: (a) along the Section 1 with Different Carburization Schedules, (b) along Three Critical Sections with 12 Hours Carburization Time.

The hardness distribution in the carburized case is normally used to check the quenching result in industry. During the DANTE simulations, the hardness is calculated based on the volume fractions of phases, carbon content, and the temperature at which the phase was formed. Figure 9 shows the comparison of the predicted hardness and the measured hardness from experiments with the 8 hours carburization time along the critical section 1. The X-axis in Figure 9 is the depth in *mm* starting from the OD surface. The Y-axis is the

hardness in Rockwell C scale. The curve with the solid diamond marks are the experimental hardness measurements, and the curve with the hollow circle marks shows the predicted hardness values. As shown in Figure 9, the experimental and predicted hardness values are closely matched. The surface hardness is mainly affected by the carbon content and the cooling rate during quenching. At depths within 0.9 *mm* of the shaft OD surface, the hardness decreases slightly with the depth, which is mainly due to the carbon decrease with the depth. Inside the carburized case, the martensite and the lower bainite are the two existing phases, and they have similar mechanical properties and hardness. At a depth deeper than 0.9 *mm*, the carbon content drops down below 0.4% and the main phase distribution shifts from either martensite or lower bainite to upper bainite. The upper bainite with low carbon has low hardness. Therefore, the hardness value starts to drop as depth exceeds 0.9 *mm*.

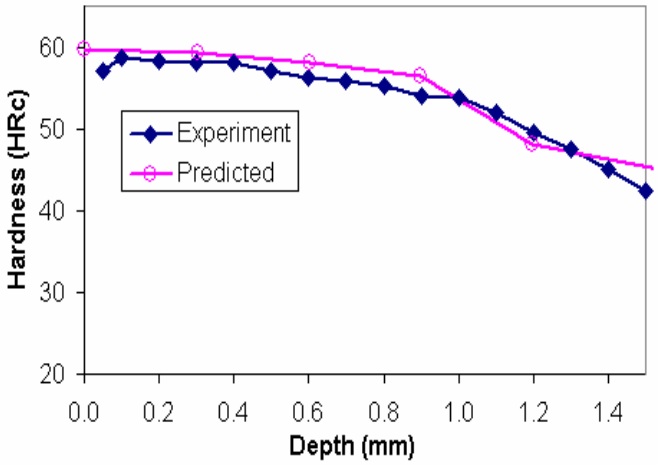

Figure 9: Comparison of Experimental and Predicted Hardness with the 8 Hours Carburization Time.

Both the thermal gradient and the phase transformations contribute to the internal stress evolution and dimensional change during the whole heat treatment process. The residual stress and dimensional change are also affected by geometry. For this transmission output shaft, DANTE predicted insignificant distortion after heat treatment, which matched the experiments. The low distortion caused by this heat treatment process removed distortion as an important issue, and therefore distortion is not discussed in this paper. Residual stress, however, is a major issue due to its impact on fatigue life.

The residual stress distributions along section 1 are shown in Figure 10(a) for the four carburization schedules. The minimum principal residual stress predicted at the surface is about 250 *MPa* in compression for all four cases. The surface residual stress has a slight increase in compression with the depth in the shallow surface as shown in the Figure 10. This is mainly caused by the phase transformation sequences shown in Figure 8. By increasing the carburization time, the depth of the compressive zone is increased. The residual stress difference between 3 hours carburization time and 8 hours carburization time is significant, as shown in Figure 10(a). However, the residual stresses difference among 8 hours, 12 hours, and 18 hours carburization time is insignificant. Higher surface residual stress in compressive is preferred to improve the fatigue life of the shaft. Considering the cost by increasing the carburization time and the residual stress requirements, a carburization time between 8 hours and 12 hours should be the optimum.

Figure 10(b) shows the residual stress distributions along the three critical sections for a 12 hour carburization time. The residual stress at the surfaces of sections 2 and 3 are slightly more compressive than that of section 1. The compressive residual stresses increase with the depth at the shallow surfaces of section 2 and section 3, which are from combined effects of thermal gradient, phase transformation sequences, and geometry.

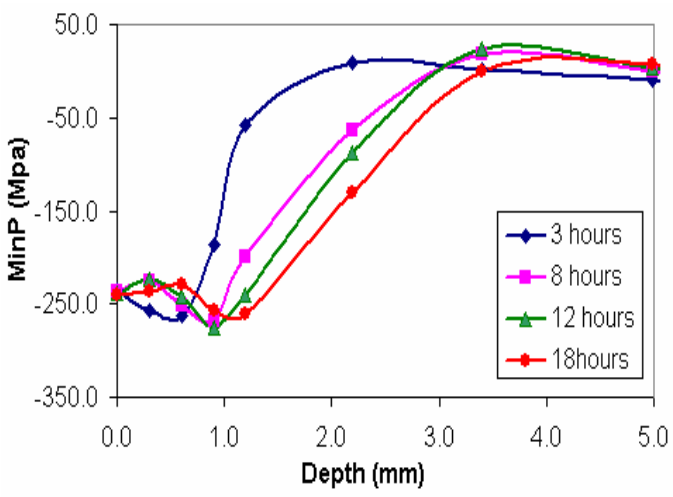

(a)

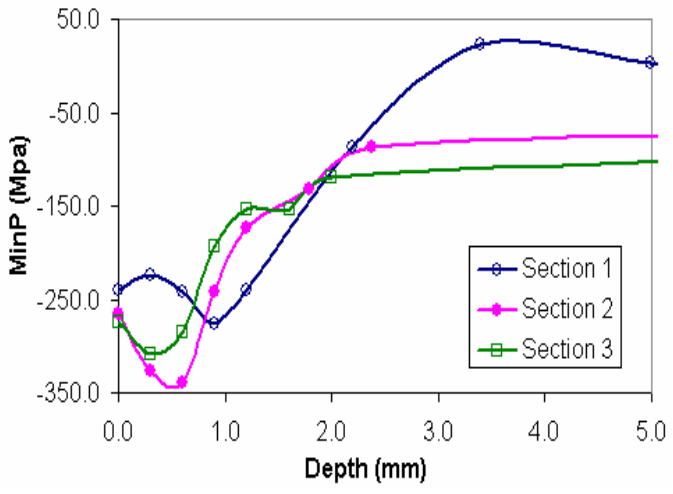

(b)

Figure 10: Minimum Principal Stress Distributions: (a) along Section 1 with Different Carburization Schedules, (b) along Three Critical Sections with 12 Hours Carburization.

Summary

The heat treatment process of a transmission output shaft was successfully simulated using the finite element software, DANTE. The complex geometry, which included a blind bore and six oil holes, was simulated using a half symmetry model. Four carburization schedules having an increase in carburization time were simulated, and the carbon profiles were predicted.

The simulations indicated that the carburization schedules had significant effects on the phase transformation sequences and internal stress evolution, with distortion for this part being a minor issue. The predicted and measured hardness distributions in the carburization case were well matched. Higher compressive residual stresses in the carburized surface are required to improve the shaft's fatigue life, and the residual stresses at three critical locations for the four carburization schedules were compared. By increasing the carburization time from 3 hours to 8 hours, the depth of the surface compressive residual stress was increased significantly. However, by increasing the carburization time from 8 hours to 18 hours, the surface residual stress distributions did not change significantly. Simulations showed that a carburization time between 8 and 12 hours is preferred, with diminishing returns in terms of improved compressive stress being achieved for times greater than 12 hours. Since fatigue life of the transmission output shaft is dependent on the level of compressive residual stress, it is expected that a carburization time between 8 and 12 hours will offer peak torsional fatigue life. Fatigue testing is in progress.

References

1. D. Bammann, et al., *"Development of a Carburizing and Quenching Simulation Tool: A Material Model for Carburizing Steels Undergoing Phase Transformations*", *Proceedings of the second International Conference on Quenching and the Control of Distortion*, 367-375, November (1996)
2. Z. Li, B. Lynn Ferguson, and A. M. Freborg, *"Data Needs for Modeling Heat Treatment of Steel Parts*", Proceedings of Materials Science & Technology Conference, 219-226, September (2004)
3. A. M. Freborg, Z. Li, B. Lynn Ferguson, and D. Schwam, "Improving the Bending Fatigue Strength of Carburized Gears", Proceedings of Materials Science & Technology Conference, 227-234, September (2004)
4. T. Inoue, and K. Arimoto, *"Development and Implementation of CAE System "HEARTS" for Heat Treatment Simulation Based on Metallo-Thermo-Mechanics*", *Journal of Materials Engineering and Performance*, 51-60, 6(1), (1997).
5. K. Arimoto, D. Lambert, and W. T. Wu, "*Finite Element Analysis of Internal Stresses in Quenched Steel Cylinders*", *Proceedings of the 19th Heat Treating Conference*, 425-434, November (1999)
6. B. Lynn Ferguson, A. Freborg, and G. Petrus, "Software Simulates Quenching", *Advanced Materials and Processes*, H31-H36, August (2000)
7. B. Lynn Ferguson, Z. Li, A. M. Freborg, "Modeling Heat Treatment of Steel Parts", *Computational Materials Science*, 274-281, 34(2005)